3.3 VALIDATION OF BOUNDARY-LAYER PARAMETERIZATIONS IN A MARITIME STORM USING AIRCRAFT DATA

P. Ola G. Persson[1], Bernard Walter[2], J-W. Bao[3], and Sara Michelson[1]

[1]Cooperative Institute for Research in Environmental Sciences/NOAA/ETL, Boulder, CO
[2]NorthWest Research Associates, Bellevue, WA
[3]NOAA/Environmental Technology Laboratory, Boulder, CO

1. INTRODUCTION

Processes both near the surface and aloft in interstorm regions of maritime extratropical cyclones can produce significant effects on the development of the systems along the storm track. Large surface fluxes in cold air outbreaks behind a passing system can play a significant role in preconditioning the atmosphere for the development of the next frontal wave, as suggested by Reed and Albright (1986). They suggest the possibility that the surface fluxes alter the low-level baroclinicity of the prestorm environment for the subsequent storm, thereby affecting its development on a 24-hour time scale. Surface heat fluxes can impact the low and mid-level stability of a storm on slightly shorter time scales, as seen for a comma cloud producing strong convection in California during the 1982/83 El Nino season (Reed and Blier 1986).

Observations obtained with the NOAA P-3 aircraft on February 6-7, 1998, during the California Landfalling Jets Experiment (CALJET; Ralph et al 1999) are used to document the processes occurring in the interstorm environment and to validate several planetary boundary layer (PBL) parameterization schemes using two methods. Off-line validation uses the observed mean flow and thermal characteristics, while 3-D modeling with the Penn State/NCAR Mesoscale Model (MM5) relies on the model atmosphere and surface characteristics. The Blackadar (Blackadar 1976; Zhang and Anthes 1982), the operational Medium Range Forecast Model (MRF) (Hong and Pan, 1996), and the Burk-Thompson (Burk and Thompson, 1989) PBL schemes are used. The first two use non-local schemes with first-order closure, while the last uses a local scheme with second-order closure. Only the 3D modeling will be presented in this paper, but the off-line results will be shown at the conference.

2. OBSERVATIONS

The NOAA P-3 aircraft obtained a north-south cross-section of the atmospheric structure and surface fluxes in the cold-air region between two large maritime cyclones off the coast of California (Fig. 1). Sensible and latent heat, and momentum fluxes were obtained from covariance calculations using 40-Hz gust-probe and fast temperature and humidity measurements in 4 flux stacks. Each flux stack consisted of three low-level legs approximately 70 km in length, with the lowest leg at 68 m above the ocean surface and the top leg near

Corresponding author: Dr. Ola Persson, CIRES/NOAA/ETL, 325 Broadway, Boulder, CO 80303. E-mail: ola.persson@noaa.gov

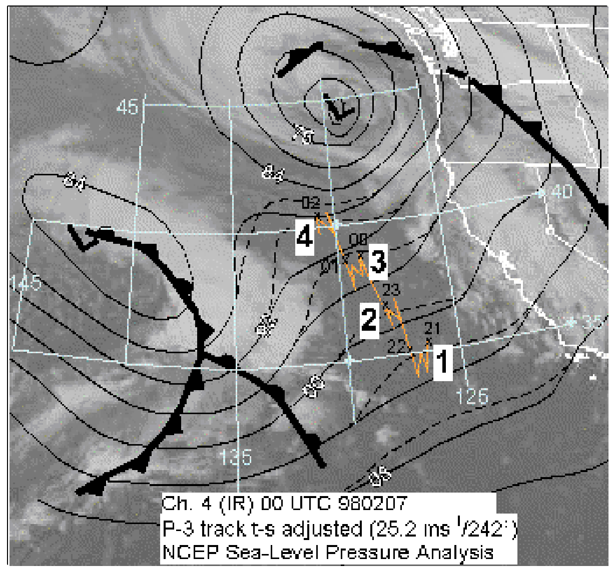

Fig. 1: *NCEP SLP analysis (solid line), P-3 flight track (grey line) and IR satellite image at 00 UTC Feb. 7, 1998. Dashed isopleths are adjustments to the SLP analysis based on the P-3 observations. The flight track has been time-to-space adjusted using a phase velocity of 25.2 ms^{-1} from 242°. The flux stacks are numbered (large numbers), and the time (UTC) along the flight track is also shown.*

the PBL top (Fig.2). The flux-stack legs were oriented approximately perpendicular to the PBL wind. Khelif *et al.* (1999) estimate the accuracy of the P-3 turbulent fluxes as ±0.015 Pa for stress, ±2.5 Wm^{-2} for sensible heat flux and ±15 Wm^{-2} for latent heat flux. The stacks were connected by slow ascent/descents up to about 500 mb and dropsonde data to give a uniquely complete structure of the lower troposphere in a cross-section perpendicular to the storm track. The northern flux stack was just SE of the main circulation of the first low, and fair-weather cumulus existed in the entire region (Fig. 1). The P-3 observations show a sea-level pressure (SLP) difference of 13.4 mb across the cross-section, and indicate that the short-wave ridge is stronger and sharper than in the NCEP analysis.

The cross-sections reveal a very weakly baroclinic lower troposphere with the only significant meridional thermal gradient occurring above 700 mb near the southern end of the cross-sections (Fig. 2a). This is also where the strongest winds were observed (Fig. 2b). Throughout the rest of the domain, winds of moderate speed were observed (14-20 ms^{-1}), with PBL winds from the WSW at the southern end and from the SW at the northern end. The outstanding features of the moisture cross-section (Fig.2c) are 1) the lack of a large-scale meridional moisture gradient below 800 mb, 2) the lack of a well-defined level for a sharp moisture gradient in the vertical, and 3) the presence of significant small-scale horizontal moisture gradients in the flux stacks, where the resolution was adequate to resolve them. These small-scale variations likely exist between the flux stacks as well. Intrusions of drier air from aloft into the PBL are seen on the scales of 10-20 km in flux stacks 2 and 3. Below approximately 750 mb, the environment was potentially unstable in the entire cross-section.

The PBL depth was estimated to correspond to the base of the significant increase in the virtual potential temperature. However, many of the ascent/descent and dropsonde profiles consisted of one to three layers of increased gradients of a few hundred meters depth before a general gradient increase began. The shallowest PBL depth was therefore assumed to be at the lowest gradient increase, while the largest PBL depth was assumed to be at the top gradient increase. The mean of the range of the PBL top was at about 864 mb (1250 m) to the south and 890 mb (900 m) to the north (Fig. 2a).

The turbulent sensible heat flux (H_S) is positive near the surface and negative in the middle and near the top

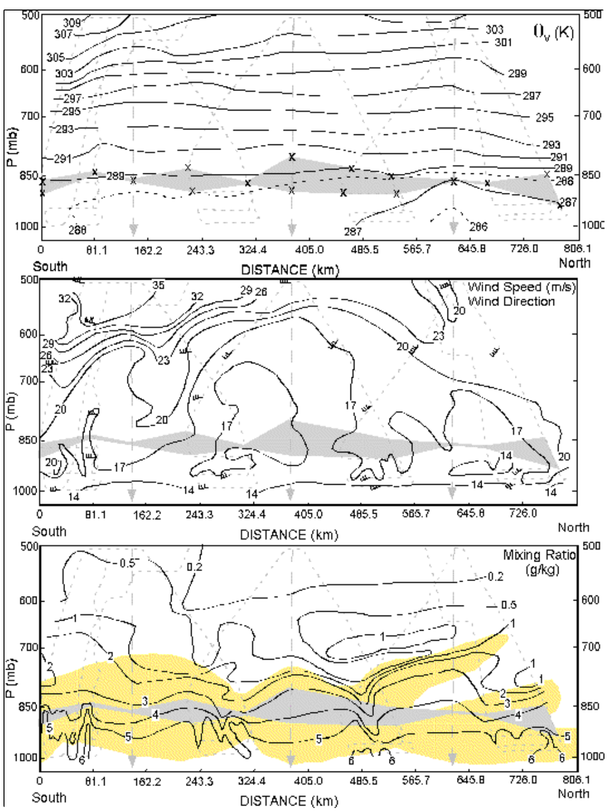

Fig. 2: *Cross-sections of a) virtual potential temperature (θ_v; K), b) isotachs and selected wind barbs (ms^{-1}), and c) mixing ratio (gkg^{-1}). The analyses were created from the in-situ data along the aircraft track (grey dashes) and the dropsondes (dashed arrows). The maximum and minimum PBL depth is shown by the dark grey zone (and x's in a)), while the region of potential instability is shown as light grey in c).*

of the PBL (Fig. 3a). The vertical flux divergence indicates weak warming by turbulence throughout the PBL, except near the surface at the very northern end. The latent heat flux (H_l) was positive throughout (indicating an upward flux of moisture) and significantly larger in magnitude than H_S. The vertical flux divergence indicates turbulent moistening in the southern end of the cross-section, especially in the upper portions of the PBL. Turbulent drying of the PBL was observed in the northern half of the cross-section, especially at low levels. Hence, the turbulent fluxes were acting to establish a moisture gradient, with greater moisture to the south than the north. The momentum fluxes (not shown) show a constant stress for the lowest two legs of each flux stack (u_*= 0.43-0.49 ms^{-1}), and smaller values at the top leg (u_*= 0.22-0.31 ms^{-1}). This is consistent with a constant flux layer in the PBL at least up to the middle leg of each stack (222 m at the northern end and 532 m at the southern end), while the PBL momentum decrease occurs in the upper portion. The turbulent kinetic energy (Fig. 3c) ranged

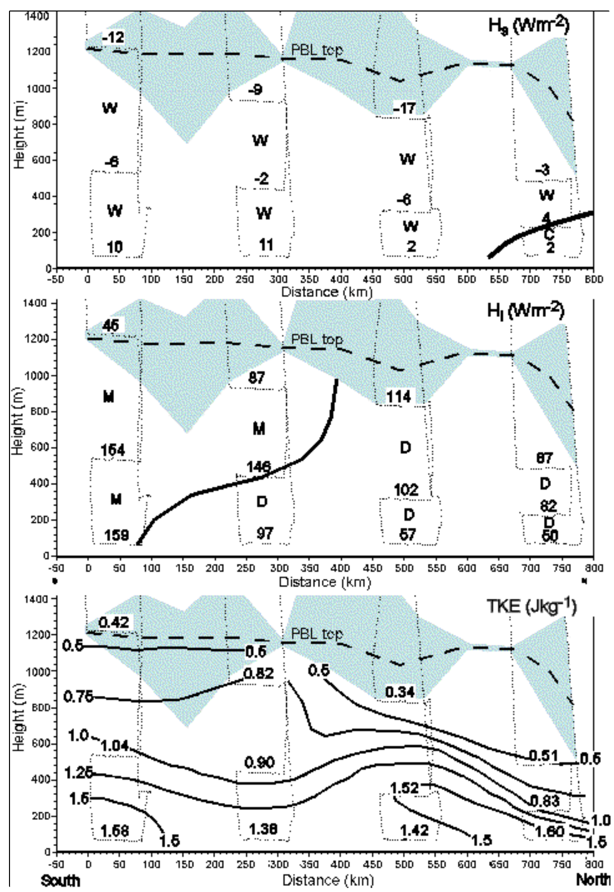

Fig. 3: *Cross-sections of a) sensible heat flux (H_s; Wm^{-2}), b) latent heat flux (H_l; Wm^{-2}), and c) turbulent kinetic energy (TKE; solid lines; Jkg^{-1}) averaged along each flux-stack leg. The heavy solid lines in a) and b) separate areas of turbulent warming (W) and cooling (C) in a) and moistening (M) and drying (D) in b). The PBL top range (grey area) and mean (heavy dashed line) are shown.*

from 1.5 Jkg^{-1} at the surface to 0.5 Jkg^{-1} near the PBL top.

3. MM5 MODELING

The three-dimensional experiments with the Penn State/NCAR Mesoscale Model (MM5) are outlined in Table 1. All experiments used a 36 km coarse mesh

Table 1: MM5 3-D experiments.

Exp. Name	SST	PBL Scheme	Precip. Param
BTE	ECMWF	Burk-Thompson	Simple ice
BLE	ECMWF	Blackadar	Mixed phase
MRE	ECMWF	MRF	Mixed phase
MRES	ECMWF	MRF	Simple ice
BTA	AVHRR	Burk-Thompson	Simple ice
MRENF	ECMWF	MRF-no heat fluxes	Mixed phase

and a nested 12 km mesh, were initialized by the ECMWF initial conditions at 12 UTC Feb. 6, and utilized the Kane-Fristch convective scheme. Fifty layers were used in the vertical, with 15 of them below 1.6 km height. The first three experiments (BTE, BLE, and MRE) show the effects of three different planetary boundary layer schemes. Because the Burk-Thompson PBL scheme currently only works when linked to the simple ice-physics grid-scale precipitation scheme, runs BTE and BTA used this precipitation scheme while the others used the mixed-phase precipitation scheme. Because no grid-scale precipitation (and very little precipitation at all) occurred in the interstorm region, this difference does not have a significant effect on the verification at the observation cross-section in the interstorm region, but does have an effect on the variations in coastal precipitation between the runs. This has been verified with experiment MRES. Experiment BTA used a SST analysis that was derived from the AVHRR observations and validated at the four flux stack points with airborne expendable bathy-thermographs (AXBTs) and radiometric measurements. The ECMWF SST analysis was 1.0-1.5°C greater at these validation points and was deemed inaccurate. These differences most likely occurred because of the use of a climatological first-guess in the ECMWF SST analysis and the presence of the extremely atypical SST distribution during this El Niño season. Experiment MRENF set all surface sensible and latent heat fluxes to zero throughout the domain, and was done to illustrate the significance of the surface heat and moisture fluxes for the coastal precipitation during landfall of the second storm.

After 12 h of Experiment BTE (00 UTC Feb. 7), storm 1 was exiting the fine-mesh domain to the north while storm 2 was entering from the west (Fig. 4). Compared to the NCEP analysis, low 1 in BTE is displaced 163 km to the southeast and 3 mb weaker,

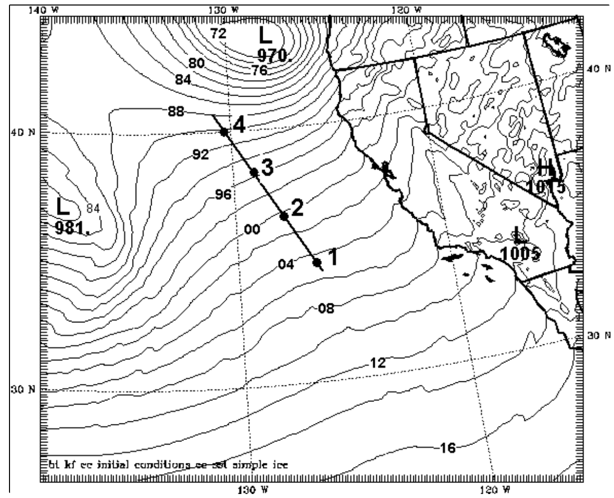

Fig.4: *Sea-level pressure analysis from Exp. BTE valid at 00 UTC Feb. 7. The geographic positions of the cross-sections in Figs. 5 and 6 (bold line) and the time-to-space adjusted flux stacks (dots) are shown.*

while storm 2 is also displaced to the southeast but of the correct magnitude. As a result, the model SLP along the flight track is about 1-1.5 mb lower than that observed by the P-3 but 0-1 mb greater than the NCEP analysis.

In good agreement with the observations, the cross-section of θ_v from BTE shows a PBL top near 860 mb (Fig. 5a). The isotach field (not shown) is also in good agreement, while the modeled moisture field has a much stronger vertical gradient at the PBL top than in the observations (Fig. 5b). This sharp gradient occurs throughout the cross-section except in the southernmost 100 km. Note that the modeled 2- degree meridional θ_v gradient in the PBL corresponds well with the observations, but the 1.5 gkg^{-1} increase from north to south in the modeled PBL is not observed. The model TKE field also has a meridional gradient that is not observed, and it is slightly weaker at the PBL top than observed (Fig. 5c). The model indicates turbulent plumes occurring on the scale of the model resolution and similar to that seen in the observed moisture field. Note that Experiment BTA is used for the TKE comparison, as this is the best simulation (see below), and we are only able to compare the TKE field when using the Burk-Thompson PBL scheme. Cross-sectional flux diagnostics are not yet available from the model.

The PBL structure of Exp. BLE is similar to BTE, except that the PBL is 15-20 mb deeper. In simulation MRES (and MRE), however, the PBL is 70-90 mb deeper and slightly warmer and drier than BTE and the observations (Fig. 6). At this point, it is unclear whether the differences between MRES and BTE (and the observations) are due to the non-local nature of the MRF scheme, its lower-order closure, or both.

The surface fluxes are significantly larger in the simulations than in the observations (Fig. 7), especially at the northern end. For H_l, one reason is the drier PBL in the simulations leading to larger vertical moisture gradients. Simulation BTA, which uses the AVHRR

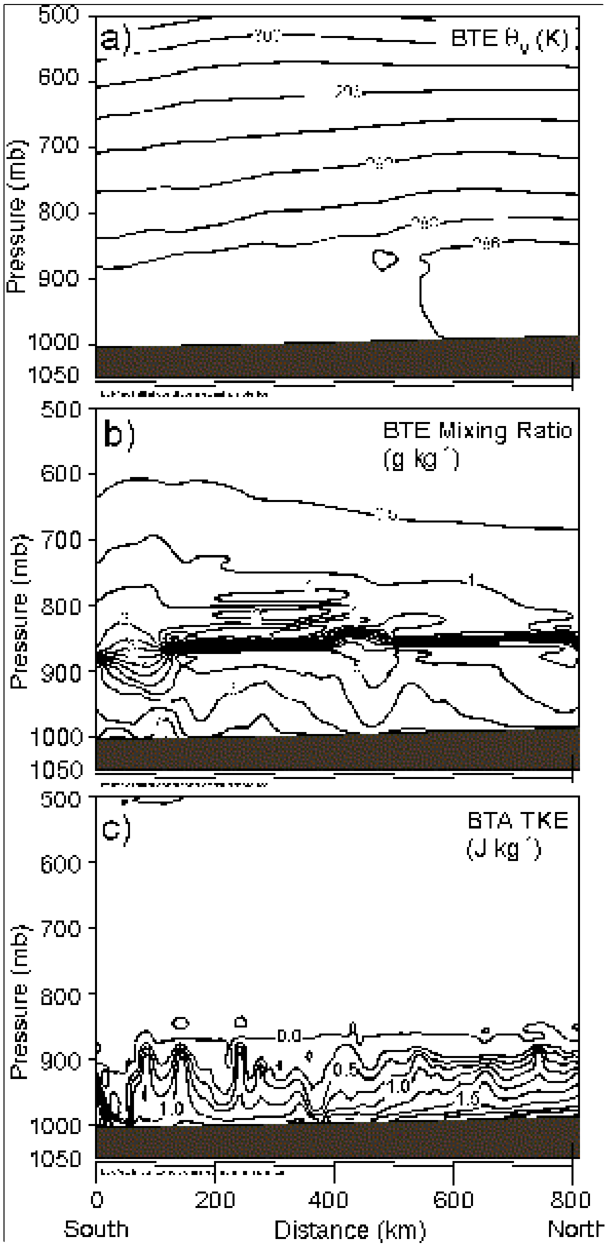

Fig. 5: *Cross-sections of a) q_v (K) from BTE, b) mixing ratio from BTE, and c) TKE (Jkg^{-1}) from BTA. The position of the cross-sections is shown in Fig. 4.*

SST analysis, shows an improvement over BTE for all fluxes, suggesting that the errors in the ECMWF SST analysis have an impact. In addition, BTA_adj adjusts the model cross-section for the position error of the modeled low center compared to the NCEP analysis. This adjustment has a significant impact on the validation of H_s, but only a minor impact on the other fluxes. All three fluxes are still too large at the northern end. In general, the fluxes from BTE are in better agreement with the observations than are those from BLE or MRE.

To illustrate the impact of the PBL schemes and surface fluxes on the precipitation from storm 2 at

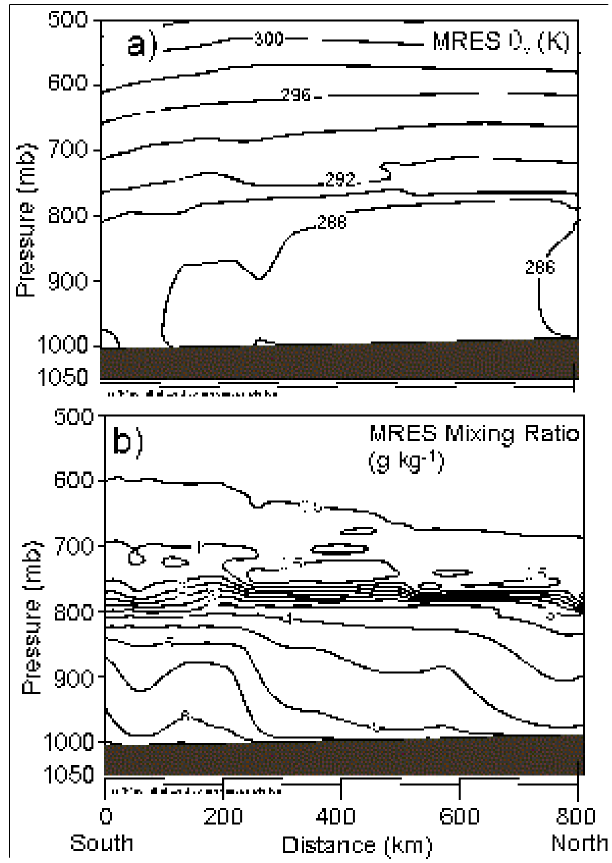

Fig. 6: *Same as for Fig. 5a and 5b, but for Exp. MRES.*

landfall, Fig. 8 shows 21 h accumulations from selected mountain sites along the California coast. The sites on the left side are in southern California and those on the right in the north. The verification time was chosen to separate the precipitation of storms 1 and 2 in both the models and the observations. The variations around the observed accumulated precipitation ranged from -1.2 - +0.81 cm (-18% - +12%) in the Santa Ynez mountains to -7.7 cm (-76%) at Three Peaks. The maximum variation between experiments (excluding MRENF) ranged from 27% at Santa Ynez and the northern end of the Central Valley to 54% at Three Peaks. Though no experiment was clearly best, the BTA simulation was no more than 1.3 cm (-17%) off at three of the sites and only 46% low at Three Peaks. Comparing simulation MRES with MRE shows that varying the PBL scheme has as much or greater impact on the precipitation as does varying the treatment of ice in the precipitation scheme. Obviously, many complex physical processes are involved in the generation of precipitation, including non-linear interactions between different model parameterizations, so a simple relationship to the PBL scheme or the ice physics scheme should not be expected.

The large decrease in precipitation in Exp. MRENF compared to MRE at Three Peaks and the Santa Ynez Mts. shows that H_s and H_l had a major impact on the precipitation in the southern coastal mountains, but not at the northern sites.

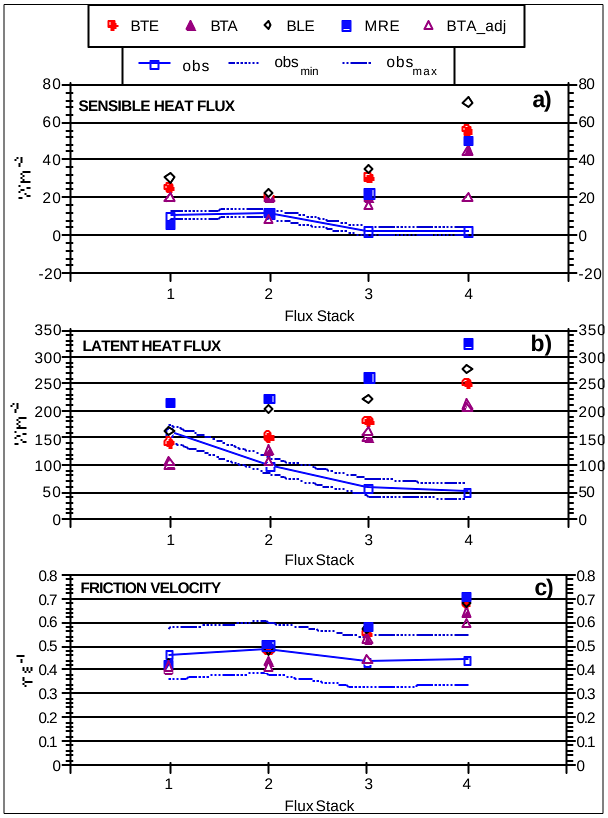

Fig. 7: *Observed (open squares) and modeled surface a) sensible heat flux, b) latent heat flux, and c) friction velocity* (u_*) *at the flux stack locations. The error range from Khelif* et al. *(1999) for the P-3 observations is shown by the dotted lines.*

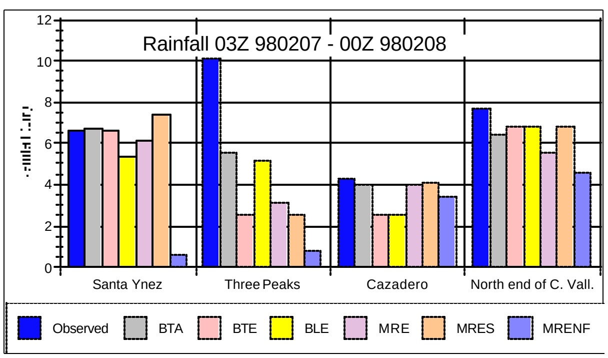

Fig. 8: *Observed and modeled accumulated precipitation at selected coastal mountain sites from 03 UTC Feb. 7 – 00 UTC Feb. 8.*

4. CONCLUSIONS

Exceptionally detailed observations of the lower tropospheric and PBL structure were obtained in the interstorm region between two major maritime cyclones. These observations have been used to validate surface flux and PBL schemes. The results show significant differences between the schemes in the offshore PBL depth and structure and in the surface heat fluxes. The precipitation in the coastal mountains varied by as much as 50% from one scheme to another. In general, the simulation using the Burk-Thompson PBL scheme and the AVHRR SST analysis performed best for this case.

The significance of the errors in the PBL structure and processes seen in the interstorm region of the simulations is, as of yet, unknown. Variation in the coastal precipitation did occur with variation in PBL scheme, and the simulation that produced the best offshore interstorm PBL structure (BTA) also produced coastal precipitation that was most similar to the observations. This suggests that there may be a link between the fidelity of the PBL structure in the offshore interstorm region in the simulations and the subsequent coastal precipitation. However, we don't know whether the processes in the interstorm region were themselves important to the coastal precipitation, or whether processes elsewhere in the storm were more important and were also affected by the PBL scheme and SST analysis used in the simulations. Further experiments using selective regional control of the surface fluxes will be attempted to answer this question. In addition, coastal precipitation may not be the best parameter for assessment of impact of offshore PBL fidelity, as it is a result of many complex processes. Other parameters also need to be examined.

REFERENCES

Blackadar, A. K., 1976: Modeling the nocturnal boundary layer. *Proceedings of the Third Symposium on Atmospheric Turbulence, Diffusion and Air Quality*, pp. 46-49, Amer. Meteor. Soc., Boston, Mass.

Burk, S. D., and W. T. Thompson, 1989: A vertically nested regional numerical prediction model with second-order closure physics. *Mon. Wea. Rev.*, **117**, 2305-2324.

Hong, S.-Y., and H.-L. Pan,1996: Nonlocal boundary layer vertical diffusion in a medium-range forecast model. *Mon. Wea. Rev.*, **124**, 2322-2339.

Khelif, D., S. P. Burns, and C. A. Friehe, 1999: Improved wind measurements on research aircraft. *J. Atmos. Oceanic Technol*., **16**, 860-875.

Ralph, F. M., P. O.G. Persson, D. Reynolds, W. Nuss, D. Miller, J. Schmidt, D. Jorgensen, J. Wilczak, P. Neiman, J.-W. Bao, D. Kingsmill, Z. Toth, C. Veldon, A. White, C. King, and J. Wurman, 1999: The California Land-falling Jets Experiment (CALJET): Objectives and design of a coastal atmosphere-ocean observing system deployed during a strong El Nino. *Preprints, 3rd Symp. on Integrated Observing Systems*., Jan. 10-15, 1999, Dallas, TX, 78-81.

Reed, R. J., and M. D. Albright, 1986: A case study of explosive cyclogenesis in the eastern Pacific. *Mon. Wea. Rev.*, **114**, 2297-2319.

Reed, R. J., and W. Blier, 1986: A further study of comma cloud development in the eastern Pacific. *Mon. Wea. Rev*. **114**, 1696-1708.

Zhang, D.-L., and R. A. Anthes, 1982: A high-resolution model of the planetary boundary layer-sensitivity tests and comparisons with SESAME-79 data. *J. Appl. Meteor.*, **21**, 1594-1609.